Susceptibility of strongly driven two-level atoms: A non-Markovian analysis

J. R. Brinati*
Instituto de Física, Universidade Federal do Rio de Janeiro, Caixa Postal 65.258, 21945-970 Rio de Janeiro, RJ, Brazil

S. S. Mizrahi† and G. A. Prataviera‡
Departamento de Física, Universidade Federal de São Carlos, Rod. Washington Luiz Km 235, São Carlos, 13565-905, SP, Brazil
(Received 31 January 1997; revised manuscript received 3 April 1997)

The absorptive part of the susceptibility of a system constituted by a strongly driven two-level atom (interacting with a reservoir) is analyzed when probed by a weak field. Memory effects are taken into account (the correlation time of the reservoir variables is finite) and we verify that they lead to several distinct features for the absorption and stimulated emission of radiation, when compared with those obtained in the Markovian approximation. Moreover, we verify that memory effects lead to a signature, namely, the sensitive dependence of the maxima of the absorption lines on the Rabi frequency at off-resonance pumping. Other characteristics of the spectrum are enhanced, even in the presence of a small but non-null correlation time of the reservoir, for instance, the maxima of the dispersionlike absorption curves at on-resonance pumping. In this work several situations are analyzed for different values of the parameters of the problem: the off-resonance frequencies of the driving field, the Rabi frequency, the memory time, and temperature of the reservoir.
[S1050-2947(97)09607-8]

PACS number(s): 32.70.Jz, 42.50.Ar

I. INTRODUCTION

It is well known that several interesting effects arise in the interaction of atoms with radiation when non-Markovian (NM) characteristics of the reservoir are assumed, and they may manifest in many physical situations. For instance, Lewenstein, Mossberg, and Glauber [1] predicted the supression of spontaneous emission related to the decay of cavity two-level atoms in the presense of a strong driving field. Other authors [2] studied NM effects in the atomic absorption band shape for the transient and steady-state regimes and concluded that no information can be obtained about the NM character of the system in the steady-state regime because the line-shape function is Lorentzian as it is in the Markovian approximation (MA); the effects are perceptible only in the transient regime, where the line shape is asymmetric. In this same line, in [3] the authors derived a NM master equation by expanding the density operator in first power in the correlation time τ of the reservoir, obtaining thus the same qualitative results as in [2], with a model-independent reservoir spectrum. Later, it was shown [4] that the intensity of the diffracted light in degenerate four-wave-mixing processes can be expressed as a simple function of the memory function of the reservoir. More recently, in [5] the transient four-wave mixing from a three-level system was examined when quantum beats and NM effects occur simultaneously; the authors showed that it is possible to distinguish between oscillations due to correlations of the reservoir from oscillations arising from quantum beats.

In previous papers [6,7] we analyzed and discussed the NM effects in driven two-level atoms in the steady-state regime. We pointed to the possibility of distinguishing solutions of the master equation under the MA from those coming from a NM treatment (NMT) with a model-dependent reservoir spectrum. We showed that the distinction occurs in the entropy function: for Markovian processes it behaves as a monotonously decreasing function of the detuning going asymptotically to a constant value, whereas in NM ones it shows a minimum before also attaining asymptotically the same value. Therefore, the presence of the minimum in the entropy function would be a signature of a NM reservoir interacting with the atom. Since the entropy function can be written in terms of the real and imaginary parts of the susceptibility, that function can be constructed from the experimental data in order to look for memory effects. Moreover, we also verified the existence of a phase transition in the absorption line shape, the transition from a single to a split peak, which depends on the temperature of the reservoir and on the correlation time of its variables.

Continuing the study on the manifestation of non-Markovian effects in the matter-radiation interaction phenomena, in this paper we analyze those in which a two-level atom is driven by a strong field, as reported in Ref. [8], where several interesting effects arise when the reservoir is assumed Markovian. For instance, a novel effect was predicted by Mollow [9] in the absorption spectrum of a probe field interacting with a system composed of a two-level atom driven by a strong laser field. This effect is the amplification of the probe field intensity by the stimulated emission from the atom at on-resonance frequencies of the strong field, $\Delta\omega \equiv \omega_1 - \omega_0 = 0$, where ω_0 is the atomic transition frequency and ω_1 is the laser frequency. Later, this effect was verified experimentally at on- and also at off-resonance frequencies, the latter case with even higher gain [10]. Theoretically, this phenomenon is viewed as an amplification

*Electronic address: brinati@if.ufrj.br
†Electronic address: salomon@power.ufscar.br
‡Electronic address: pgap@iris.ufscar.br

without population inversion in the atomic bare state picture; in the dressed state picture the amplification occurs due to emission from a population inversion in the levels, for $\Delta\omega>0$. Besides, at on-resonance pumping the amplification occurs near the absorption since the curve shows a small dispersionlike shape, which decreases as one increases the Rabi frequency (Ω); this ''anomalous'' behavior was discussed in [11].

In this work we verify that the NM character of the reservoir affects significantly the whole probe absorption spectrum χ'': at the on-resonance pumping, the dispersionlike shapes in the probe field, tuned in the neighborhood of the frequency $(\omega_1+\Omega)$, are enhanced proportionally to the increase of the Rabi frequency; this is contrary to what occurs in the MA. This enhancement occurs even for a very small memory time. At off-resonance pumping, the left-side band of the spectrum shows a behavior that can be characterized as a signature of memory effects: when, at a given Rabi frequency, the maxima of the absorption lines are plotted against the detuning $\Delta\omega$, one notes that the curve shows a maximum before decreasing to a constant value; in the MA this curve increases and then saturates at this same value without passing through a maximum. In the right-side band of the spectrum one verifies that the amplification by stimulated emission in the NMT is enhanced when compared to the case of MA, but both spectra have similar behaviors in this band. All these effects persist when the temperature of the reservoir is not null, although the intensities are attenuated. However, as already noted in [7], here too the absorption line shape of the probe presents a splitting at a critical temperature.

The presentation and discussion of these effects in the paper are organized as follows: in Sec. II we present the modifications that arise in the generalized master equation (GME) due to the presence of the probe field and in Sec. III we give its solution. In Sec. IV we derive the susceptibility corresponding to the probe and discuss the behavior of its absorptive part; Sec. V contains a summary and conclusions. Finally, in the Appendix we present the relation between nonlinear optics (field-dependent susceptibility) and the structure of the polarization vector derived from the GME.

II. THE GENERALIZED MASTER EQUATION

Firstly, we consider a system of noninteracting two-level atoms coupled to a reservoir and driven by a strong classical monochromatic field $\mathbf{E}_1(t)$. The excited and ground states are represented by the states $|1\rangle$ and $|2\rangle$, respectively, and ω_0 is the atomic transition frequency. The reservoir is, as usual, assumed to be constituted by a very large number of photons in thermal equilibrium at some temperature T. The atom-field interaction, in the rotating-wave approximation (RWA), is given by $(F_1 e^{i\omega_1 t}|2\rangle\langle 1|+\text{H.c.})$, where $F_1=-\boldsymbol{\mu}_{12}^*\cdot\boldsymbol{\varepsilon}_1^*$, $\boldsymbol{\mu}_{12}$ is the matrix element of the electric dipole moment of the atom between the excited and ground states, ω_1 is the frequency of the laser field, and ε_1 is its amplitude.

For this system the reduced density matrix can be expanded in terms of the complete set of operators that span the Hilbert space,

$$\hat{\rho}_0(t)=W_1(t)|1\rangle\langle 1|+W_2(t)|2\rangle\langle 2|+W_3(t)|1\rangle\times\langle 2|+W_4(t)|2\rangle\langle 1|, \tag{1}$$

where the coefficients $W_1(t)$ and $W_2(t)$ are the occupation probabilities of the levels subject to the normalization condition $W_1(t)+W_2(t)=1$. The coefficients of coherence, $W_3(t)$ and $W_4(t)$, have a complex conjugate relation, $W_4=W_3^*$. With the decomposition (1) the GME satisfied by $\hat{\rho}_0(t)$ [6] is transformed into the following system of coupled equations for the coefficients W_j:

$$\dot{W}_j(t)=\sum_{k=1}^{2}\int_0^t dt' Q_{jk}(t,t')W_k(t')-(-1)^j[iF_1 e^{i\omega_1 t}W_3(t)+\text{c.c.}],\quad j=1,2 \tag{2}$$

and

$$\dot{W}_3(t)=\int_0^t dt' Q_{33}(t,t')W_3(t')+i(F_1 e^{i\omega_1 t})^*\times[W_1(t)-W_2(t)]-i\omega_0 W_3(t), \tag{3}$$

given in the Schrödinger representation. The occupation probability kernels are

$$Q_{jk}(t,t')=-2(-1)^{j+k}\sum_m |K_m(\omega_m)|^2[\overline{n}(\omega_m)+\delta_{k1}]\times\cos[(\omega_0-\omega_m)(t-t')],\quad j,k=1,2 \tag{4}$$

and the coherence kernels are

$$Q_{33}(t,t')=-\sum_m |K_m(\omega_m)|^2[2\overline{n}(\omega_m)+1]e^{-i\omega_m(t-t')}, \tag{5}$$

and $Q_{44}(t,t')=Q_{33}(t,t')^*$. In the above expressions $\overline{n}(\omega_m)=(e^{\hbar\omega_m/k_B T}-1)^{-1}$ is the mean number of photons of the reservoir with frequency ω_m, k_B is the Boltzmann constant, T is the absolute temperature, and the K_m (K_m^*) are the coupling parameters related to the atom-reservoir interaction.

The stationary solutions for Eqs. (2) and (3), W_j^∞, $j=1,4$, were already determined in both the MA [9] and NM [6] cases and [6] presents the general expression for them. It is worth recalling that whereas W_1^∞ and W_2^∞ are time-independent quantities, W_3^∞ and W_4^∞ are time dependent, their steady state is driven by the oscillation of the field, namely, $W_3^\infty=\overline{W_3^\infty}e^{-i\omega_1 t}$ and $W_4^\infty=\overline{W_4^\infty}e^{i\omega_1 t}$.

Now, we consider the driven atomic system probed by a weak field, in whose susceptibility we are interested. Its interaction with the atom is given by $(F_2 e^{i\omega_2 t}|2\rangle\langle 1|+\text{H.c.})$, where $F_2=-\boldsymbol{\mu}_{12}^*\cdot\boldsymbol{\varepsilon}_2^*$, ω_2 is the frequency of the probe, and ε_2 is its amplitude satisfying the condition $|\varepsilon_2|\ll|\varepsilon_1|$.

Since the probe is a perturbing field, its effect on the density matrix of the driven atom in the steady state corresponds to a small correction; thus we write the total density matrix as

$$\hat{\rho}(t)=\hat{\rho}_0^\infty+\Delta\hat{\rho}(t), \tag{6}$$

or, making explicit the corrections for each component of the expansion (1),

$$\hat{\rho}(t)=[W_1^{\infty}+\Delta W_1(t)]|1\rangle\langle 1|+[W_2^{\infty}+\Delta W_2(t)]|2\rangle\langle 2| +[\overline{W_3^{\infty}}e^{-i\omega_1 t}+\Delta W_3(t)]|1\rangle\langle 2|+[\overline{W_4^{\infty}}e^{i\omega_1 t} +\Delta W_4(t)]|2\rangle\langle 1|. \quad (7)$$

Then, the GME for $\hat{\rho}(t)$, written in terms of the expansion components, turns into four coupled c-number integrodifferential equations,

$$\frac{d}{dt}[W_j^{\infty}+\Delta W_j(t)]=\sum_{k=1}^{2}\int_0^t dt' Q_{jk}(t,t')[W_k^{\infty}+\Delta W_k(t')] -(-1)^j\{i(F_1e^{i\omega_1 t}+F_2e^{i\omega_2 t}) \times[\overline{W_3}(t)e^{-i\omega_1 t}+\Delta W_3(t)]+\text{c.c.}\}, \quad j=1,2, \quad (8)$$

$$\frac{d}{dt}[\overline{W_3^{\infty}}e^{-i\omega_1 t}+\Delta W_3(t)] =\int_0^t dt' Q_{33}(t,t')[\overline{W_3^{\infty}}e^{-i\omega_1 t'}+\Delta W_3(t')]+i(F_1e^{i\omega_1 t} +F_2e^{i\omega_2 t})^*\{[W_1^{\infty}+\Delta W_1(t)]-[W_2^{\infty}+\Delta W_2(t)]\} -i\omega_0[\overline{W_3^{\infty}}e^{-i\omega_1 t}+\Delta W_3(t)], \quad (9)$$

and

$$\frac{d}{dt}[\overline{W_4^{\infty}}e^{i\omega_1 t}+\Delta W_4(t)]=\frac{d}{dt}[\overline{W_3^{\infty}}e^{-i\omega_1 t}+\Delta W_3(t)]^*. \quad (10)$$

III. THE SOLUTION TO THE GME

Before calculating the corrections to the coefficients, $\Delta W_j(t)$, we point out that in the Appendix we determined their time behavior by exploring the properties of the polarization of the medium in the presence of a weak probe field. The expressions given by Eqs. (A11) and (A12) for the $\Delta W_j(t)$ are formally the same as those proposed in [9]:

$$\Delta W_1(t)=\delta W_1+\eta e^{-i\Delta\nu t}+\eta^* e^{i\Delta\nu t},$$
$$\Delta W_2(t)=-\delta W_1-\eta e^{-i\Delta\nu t}-\eta^* e^{i\Delta\nu t}, \quad (11)$$
$$\Delta W_3(t)=e^{-i\omega_1 t}(\delta W_0+\delta W_+ e^{-i\Delta\nu t}+\delta W_-^* e^{i\Delta\nu t}),$$
$$\Delta W_4(t)=e^{i\omega_1 t}(\delta W_0^*+\delta W_+^* e^{i\Delta\nu t}+\delta W_- e^{-i\Delta\nu t}),$$

where $\Delta\nu=\omega_2-\omega_1$ is the detuning of the probe from the driving field frequency.

Introducing the quantities $\Delta W_j(t)$, given by Eqs. (11), into Eqs. (8)–(10) and equating the coefficients of the same exponential functions to the lowest order in the probe field strength, one gets the following equations for the unknown parameters of the Eqs. (11):

$$[-i\Delta\nu+\Lambda(\Delta\nu)]\eta-iF_1\delta W_+ +iF_1^*\delta W_-=-iF_2^*(\overline{W_3^{\infty}})^*, \quad (12)$$

$$[i\Delta\nu+\Lambda^*(\Delta\nu)]\eta^*+iF_1^*\delta W_+^*-iF_1\delta W_-^*=iF_2\overline{W_3^{\infty}}, \quad (13)$$

$$\Lambda(0)\delta W_1+iF_1^*\delta W_0^*-iF_1\delta W_0=-(iF_2^*\delta W_+^*-iF_2\delta W_+), \quad (14)$$

$$Z^*(\omega_1,\Delta\omega)\delta W_0-i2F_1^*\delta W_1-i2F_2^*\eta^*=0, \quad (15)$$

$$[i\Delta\nu-Z^*(\omega_2,\Delta\omega)]\delta W_+ +i2F_1^*\eta=-iF_2^*(W_1^{\infty}-W_2^{\infty}), \quad (16)$$

$$[-i\Delta\nu-Z^*(\omega_1-\Delta\nu,\Delta\omega)]\delta W_-^*+i2F_1^*\eta^*=0, \quad (17)$$

where $\Delta\omega=\omega_1-\omega_0$ is the detuning of the driving field frequency from the atomic transition frequency. In the above equations

$$Z(x,\Delta\omega)=i\Delta\omega-\tilde{Q}_{33}^*(-ix), \quad (18)$$

$$\Lambda(y)=-\tilde{Q}_{11}(-iy)+\tilde{Q}_{12}(-iy), \quad (19)$$

where $\tilde{Q}_{33}$ is the Laplace transform of the coherence kernel [6]

$$\tilde{Q}_{33}(p)=-\int_0^{\infty}d\omega' g(\omega')|K(\omega')|^2[2\overline{n(\omega')}+1]\frac{1}{p+i\omega'} \quad (20)$$

and $\tilde{Q}_{11}$ and $\tilde{Q}_{12}$ are the Laplace transform of the occupation probability kernels [6]

$$\tilde{Q}_{jk}(p)=-2(-1)^{j+k}\int_0^{\infty}d\omega' g(\omega')|K(\omega')|^2 \times[\overline{n(\omega')}+\delta_{k1}]\frac{p}{p^2+(\omega_0-\omega')^2}. \quad (21)$$

To determine the parameters η, δW_+, and δW_- we solve the system composed of Eqs. (12), (16), and the complex conjugate of Eq. (17). To get the remaining parameters δW_0 and δW_1 we work with Eqs. (14), (15), and the complex conjugate of Eq. (15).

In Eqs. (20) and (21) the function $g(\omega')$ is the density distribution function for the frequencies of the reservoir's photons, whose shape determines the character of the evolution of the reduced density operator. For $g(\omega')$ a constant for all frequencies, the reservoir operators are Markovian correlated, whereas for $g(\omega')$ not a constant the operators become non-Markovian correlated. In this work we adopt for $g(\omega')$ the Cauchy distribution

$$g(\omega')=g_0\frac{1}{1+(\omega'-\omega_0)^2\tau^2}, \quad (22)$$

where τ is the memory time. With this choice, for the quantities $\tilde{Q}_{33}(p)$ and $\Lambda(p)$ we get

$$\tilde{Q}_{33}(p) = -\gamma[\overline{n}(\omega_0) + 1/2]\frac{1}{1+(p+i\omega_0)\tau} \tag{23}$$

and

$$\Lambda(p) = \gamma[2\overline{n}(\omega_0) + 1]\frac{1}{1+p\tau}, \tag{24}$$

where $\gamma \equiv 2\pi g_0 |K(\omega_0)|^2$ is the natural damping constant of the atom.

IV. THE SUSCEPTIBILITY CORRESPONDING TO THE PROBE

The susceptibility with respect to the probe field, determined in the Appendix, Eq. (A15), is

$$\delta A_+(\omega_1, \omega_2, \boldsymbol{\varepsilon}_1) = -\delta W_+ \frac{N}{\boldsymbol{\epsilon}_0}\frac{|\boldsymbol{\mu}_{12}|^2}{3F_2^*}, \tag{25}$$

where the quantity δW_+, solution to Eqs. (12), (16), and (17), is written as

$$\delta W_+ = -i\frac{F_2^*}{f(-i\Delta\nu)}(W_2^\infty - W_1^\infty)\left[2|F_1|^2\left(1 - \frac{-i\Delta\nu + Z(\omega_1 - \Delta\nu, \Delta\omega)}{Z(\omega_1, \Delta\omega)}\right) + [-i\Delta\nu + \Lambda(\Delta\nu)][-i\Delta\nu + Z(\omega_1 - \Delta\nu, \Delta\omega)]\right], \tag{26}$$

with

$$f(-i\Delta\nu) = 2|F_1|^2\{[-i\Delta\nu + Z(\omega_1 - \Delta\nu, \Delta\omega)] + [-i\Delta\nu + Z^*(\omega_2, \Delta\omega)]\} + \{[-i\Delta\nu + Z(\omega_1 - \Delta\nu, \Delta\omega)][-i\Delta\nu + Z^*(\omega_2, \Delta\omega)][-i\Delta\nu + \Lambda(\Delta\nu)]\}. \tag{27}$$

In Eq. (26) $(W_2^\infty - W_1^\infty)$ represents the difference between the populations of the driven atom levels and was already determined for both the MA and the NMT, in [6], Eq. (19a).

Now, we shall analyze the imaginary part of the dimensionless susceptibility $\chi''(\Delta\nu\gamma^{-1}) \equiv \mathrm{Im}\ \delta A_+(\omega_1, \omega_2, \boldsymbol{\varepsilon}_1)/\gamma$, where the positive (negative) part of the spectrum corresponds to absorption (emission) of radiation by the atom. Besides the one-photon process, the occurrence (at off-resonance) of a stimulated emission at the right-side band of the spectrum was recognized; it is currently interpreted as a three-photon process, involving the absorption by the atom of two ω_1 photons from the driving field and the emission into the probe field of one photon of lower frequency. This can also be viewed as an amplification (of the probe field) without population inversion in the atomic bare state basis, or amplification with population inversion in the dressed state basis [10,8], for $\Delta\omega > 0$.

In Figs. 1–10 we assign several values for the Rabi frequency $\Omega \equiv 2|F_1|$ $(\hbar = 1)$ as well as for $\Delta\omega$; we also consider the effect of temperature by setting $\overline{n} = 6$, besides the case $\overline{n} = 0$ $(T = 0$ K). The memory effects are introduced by assuming for the correlation time τ (in units of natural decay time) the value $\tau\gamma = 0.2$. We recall that this problem was already investigated [9–11], however, only in the MA and for $T = 0$ K.

We first give attention to the situation where the field $\mathbf{E}_1$ is resonant with the two-level atom, $\Delta\omega = 0$ (Figs. 1–4), whose curves are symmetric for $\Delta\nu$. The MA and $\overline{n} = 0$ case (Fig. 1) shows that for low Rabi frequencies there is a strong absorption around $\Delta\nu = 0$. On increasing Ω, there is practically neither absorption nor emission; χ'' shows only quite small dispersionlike shapes at $\Delta\nu$ around the Rabi frequency [9]. Within the NMT, $(\tau \neq 0)$, significant changes occur as can be verified in Fig. 2; with increasing Ω an enhancement in the intensity of the ''anomalous'' dispersionlike shape occurs at $\Delta\nu \approx \Omega$, having approximately the same intensity for both the absorption and emission neighbor lines. Moreover, with increasing Ω a narrowing of the lines is verified and for low values of Ω the stimulated emission is absent, as in the MA. When a non-null temperature is considered, in the MA χ'' is significantly reduced; see Figs. 1 and 3. In the NMT (Fig. 4) the lines are also reduced by a factor of order $(2\overline{n} + 1)$, and we observe a broadening of the widths in the dispersionlike shapes; compare with Fig. 2. Moreover, the lines become narrower with the increase of Ω. Another interesting feature is observed in Fig. 4 for low values of Ω, the central peak of absorption is split (we recall that the curve is symmetric), which is identified by the depression of

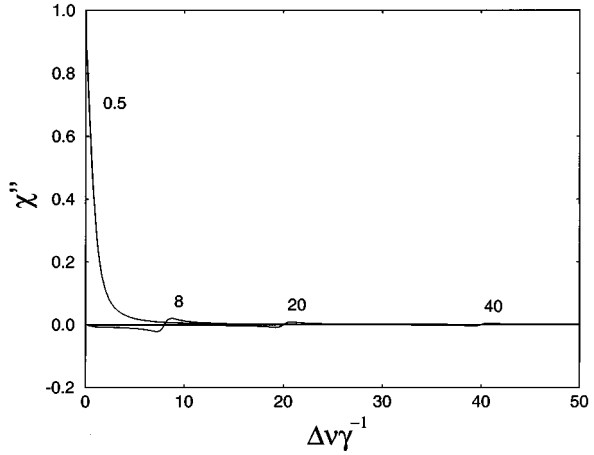

FIG. 1. Imaginary part of the dimensionless susceptibility is plotted vs the detuning $\Delta\nu$ in units of the natural decay constant, calculated in the MA $(\tau = 0)$, for on-resonance pumping, $\Delta\omega = 0$, and $\overline{n} = 0$. The numbers associated with each curve represent the Rabi frequency. The dispersionlike structure of the spectrum is quite imperceptible.

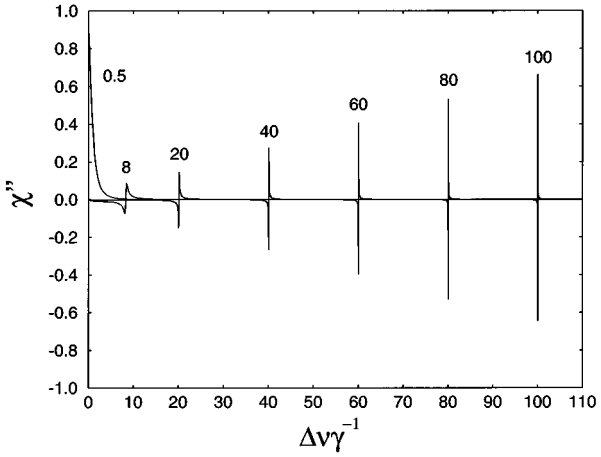

FIG. 2. Same as Fig. 1 but in the NMT, with $\tau\gamma^{-1}=0.2$. The dispersionlike shapes are enhanced compared to the MA case.

χ'' at $\Delta\nu=0$. As discussed previously [7], the reservoir is competing with the probe field for the photon absorption by the atoms; nearby $\omega_1=\omega_2=\omega_0$ the mean number of photons of the reservoir $dN=\overline{n}(\omega_0)g(\omega_0)d\omega$ is maximum; therefore the atom eventually absorbs more photons from the reservoir.

With regard to the off-resonance spectrum (Figs. 5–10) we assigned the values $\Delta\omega\gamma^{-1}=3,10,20,30,\ldots$ and $\Omega\gamma^{-1}=8$ (for higher values of the Rabi frequency we did not find significant qualitative changes). In Figs. 5 and 6 we depict χ'' in the MA and $\overline{n}=0$ for $\Delta\nu<0$ and $\Delta\nu>0$, respectively. For $\Delta\nu<0$ only absorption occurs; its intensity increases with increasing $\Delta\omega$ and then saturates. For $\Delta\nu>0$ the stimulated emission occurs but at a much lower strength than the absorption, as already noted [9,10]. The χ'' in the NMT and $\overline{n}=0$ is depicted in Figs. 7 and 8; for $\Delta\nu<0$ the heights of the absorption peaks attain their maximum around $\Delta\omega\gamma^{-1}=10$ and then decrease, saturating at the same value as in the MA (Fig. 5). This kind of behavior constitutes a signature of the memory effects in an experimental observation. Concerning $\Delta\nu>0$ (Fig. 8) the behavior of the emission line does not change when compared with

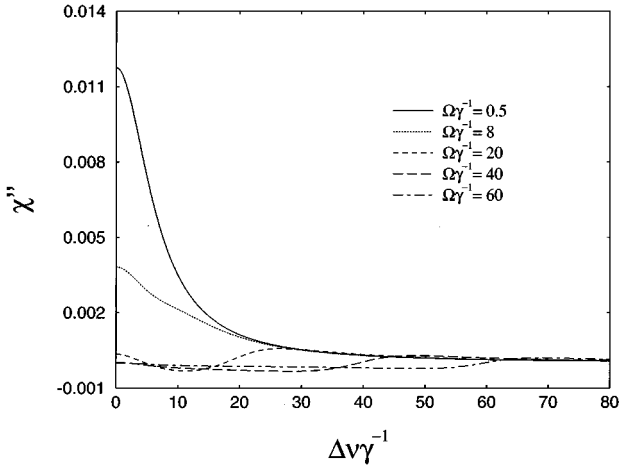

FIG. 3. Same as Fig. 1 but with $\overline{n}=6$.

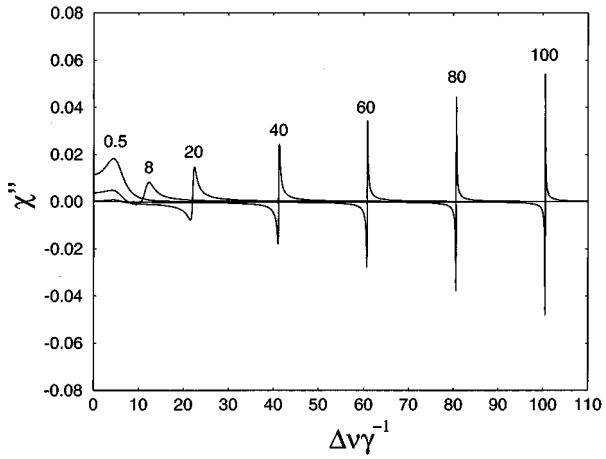

FIG. 4. Same as Fig. 1 but in the NMT with $\tau\gamma^{-1}=0.2$ and $\overline{n}=6$. The dispersionlike shapes are enhanced compared to the MA case.

the one obtained in the MA (Fig. 6) except for the strength of the emission lines whose peak is enhanced.

Concerning the effects of the temperature, $\overline{n}=6$, in the MA (Fig. 9), one notes that the main differences from the $\overline{n}=0$ case (Fig. 5) are the broadening of the linewidths and the reduction of their strengths. For $\Delta\nu>0$ the stimulated emission is highly reduced, hence we omitted this part of the plot. In the NMT (Fig. 10), we observe a significant difference by comparing to the $\overline{n}=0$ case (Fig. 7). The lines present a splitting that is independent of $\Delta\omega$. Each split line becomes asymmetric and this feature is more pronounced the lower the detuning $\Delta\omega$; for increasing $\Delta\omega$ the asymmetry tends to disappear, although the splitting persists — the lower peak increases in intensity whereas the higher one has its height decreased. Another characteristic is that for high values of $\Delta\omega$ the height of the peak, in the MA (Fig. 9) coincides with the minimum of the splitting, as already veri-

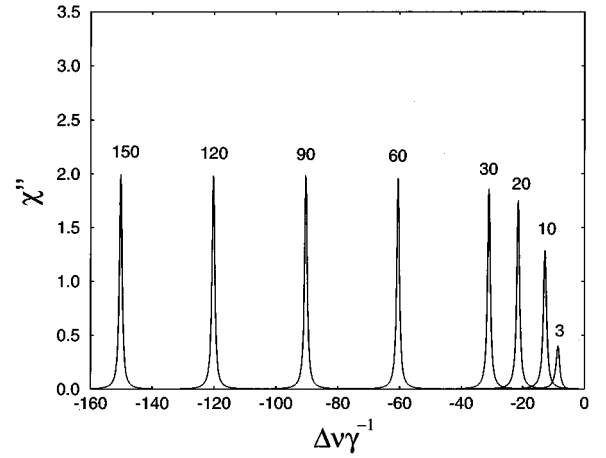

FIG. 5. Imaginary part of the dimensionless susceptibility is plotted vs the negative sideband detuning $\Delta\nu$ in units of the natural decay constant, calculated in the MA with the same value of the Rabi frequency, $\Omega=8.0$, for all absorptive curves and $\overline{n}=0$. The numbers associated with each curve represent the off resonance $\Delta\omega$.

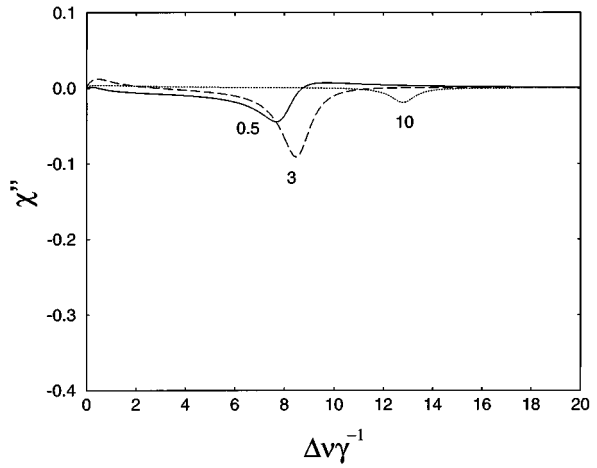

FIG. 6. Same as Fig. 5 but for positive sideband detuning $\Delta\nu$. The negative peaks correspond to the amplification of the probe by stimulated emission.

fied [7] in the case of absorption from the driving field in the absence of a probe.

V. COMMENTS AND SUMMARY

Recalling that in the dressed atom formalism [8], for $\Delta\omega>0$, the absorption and emission occur between levels at transition frequencies $\omega_0'=\omega_1-\sqrt{(\Delta\omega)^2+\Omega^2}$ and $\omega_0''=\omega_1+\sqrt{(\Delta\omega)^2+\Omega^2}$, respectively, the NM behavior of the lines can be physically understood by looking at the reservoir distribution function of frequencies, Eq. (22). At the absorption frequency ω_0', $g(\omega)$ depends only on the frequencies $\Delta\omega$ and Ω,

$$g(\omega_0')=g_0\frac{1}{1+[\sqrt{(\Delta\omega)^2+\Omega^2}-\Delta\omega]^2\tau^2}. \tag{28}$$

At on-resonance frequency, $\Delta\omega=0$, the NMT dispersionlike lines (Figs. 2 and 4) increase in intensity for high values

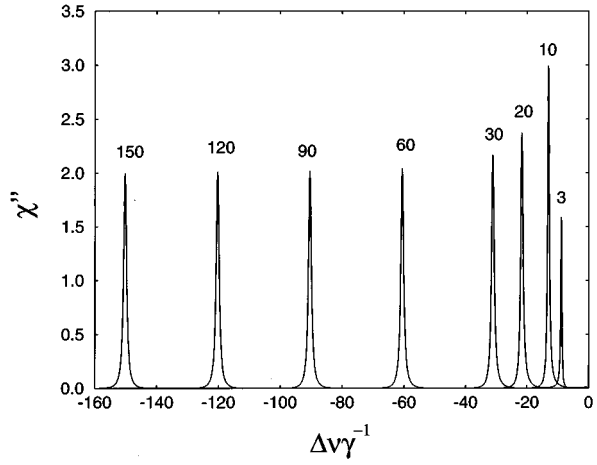

FIG. 7. Same as Fig. 5 but for calculation in the NMT, $\tau\gamma^{-1}=0.2$. After attaining values higher than in the MA, the maxima decrease with increasing $\Delta\omega$ and saturates at the same values; compare with Fig. 5.

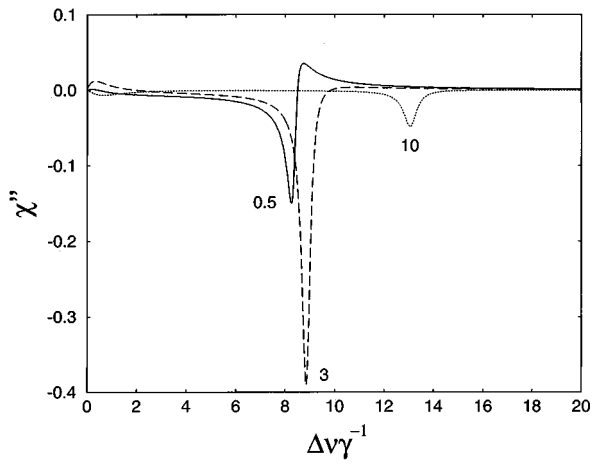

FIG. 8. Positive sideband detuning of Fig. 7. Compare the emission peaks with those of Fig. 6.

of the Rabi frequency, as compared with the ones obtained in the MA (Figs. 1 and 3), which, oppositely, decrease. This feature is present for any value of τ, however small it is, as seen from Fig. 11, whose curves (for each value of $\tau\gamma^{-1}$) represent the maxima of the absorption lines versus the Rabi frequency. In this case, $g(\omega_0')$ reduces to

$$g(\omega_0')=g_0\frac{1}{1+\Omega^2\tau^2}, \tag{29}$$

and by increasing the Rabi frequency Ω, $g(\omega_0')$ decreases, thus *reducing substantially* the influence of the reservoir on the atom-field system. The dispersionlike structure of χ'' will characterize an *almost lossless process*: the lines become quite sharp and narrow, and the intensities increase linearly with Ω.

At off-resonance frequency, $\Delta\omega\neq0$, in the MA (Figs. 5 and 9) the absorption peaks (for Ω fixed) occur at values $\omega_2=\omega_0'$ ($<\omega_0$), or $(\Delta\nu)_{\max}=-\sqrt{(\Delta\omega)^2+\Omega^2}$; the atom will also absorb photons from the pump field (which is much stronger than the probe), as long as $\Delta\omega/\Omega$ is not too large. However, as $\Delta\omega$ increases

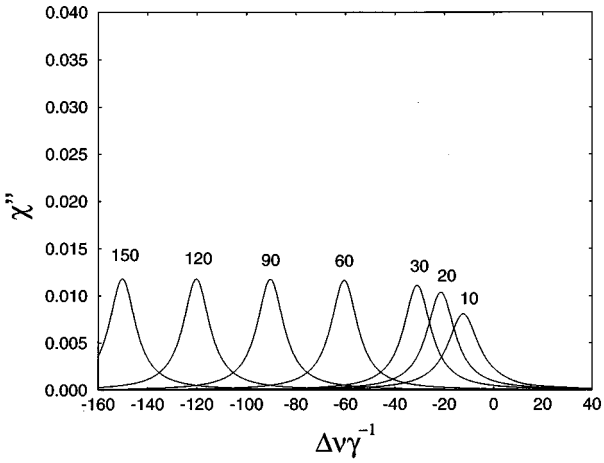

FIG. 9. Same caption as Fig. 5 but with $\bar{n}=6$. There is a broadening of the absorption lines and a decrease in their intensity when compared with those of Fig. 5.

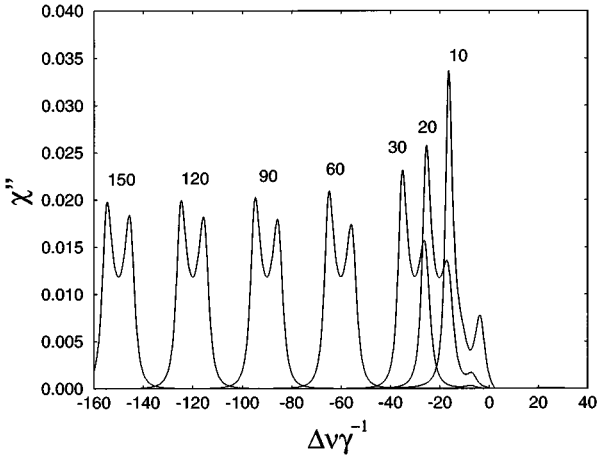

FIG. 10. Same as Fig. 5 but for calculation in the NMT, $\tau\gamma^{-1}=0.2$ and $\bar{n}=6$. Note the splitting of the line; after attaining values higher than in the MA, the maxima of the higher peak decrease with increasing $\Delta\omega$ whereas the maxima of the lower peak increase. For high $\Delta\omega$ the two peaks of the line attain the same value.

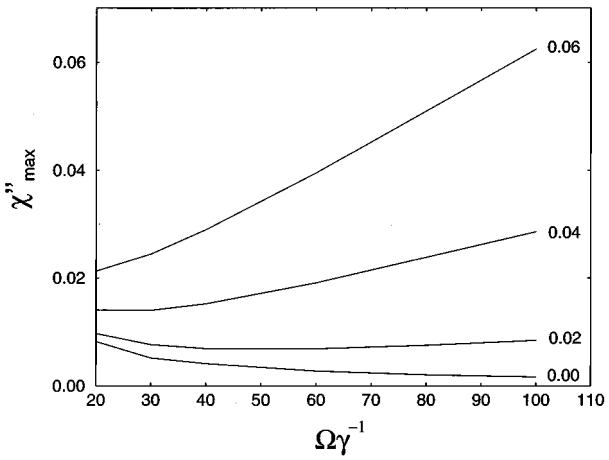

FIG. 11. Maxima of the dispersionlike shapes of Figs. 1 and 2 are plotted vs the Rabi frequency in units of the natural decay constant, for $\tau\gamma^{-1}=0.0, 0.02, 0.04, 0.06$, showing that only in MA, $\tau\gamma^{-1}=0.0$, the heights of the peaks decrease for high values of the Rabi frequency.

$$\omega_0' \equiv \omega_0 - [\sqrt{(\Delta\omega)^2+\Omega^2} - \Delta\omega] \rightarrow \omega_0,$$

the absorption from the probe attains its maximum value because the frequency ω_1 is now quite far from ω_2 and the pump field does not compete, anymore, for the absorption; this leads to the saturation of the line intensities of the probe. In the NMT (Fig. 7) the saturation of the absorption peaks occurs at the same values as in the MA because as $\Delta\omega$ becomes much larger than Ω,

$$g(\omega_0') \approx g_0 \frac{1}{1+\Omega^4\tau^2/(\Delta\omega)^2} \approx g_0 \tag{30}$$

approaches the MA in this limit. For $\Delta\omega$ of the same order of Ω, $g(\omega_0')<g_0$, the effect of the reservoir is reduced, hence increasing the absorption from the probe. The absorption lines in the NMT, when compared with the MA ones in this region, appear, each one multiplied by a factor larger than 1; the rate at which these factors decrease as $\Delta\omega$ increases provides the structure of the maximum for the peak values. We consider that this behavior characterizes a signature of the memory effects.

For $T\neq 0$, the absorption line structure for the NMT (Fig. 10) reproduces the corresponding one for $T=0$ (Fig. 7), although now each line is split because $\tau\gamma(2\bar{n}+1)>1$ [for $\tau\gamma(2\bar{n}+1)<1$ there is no split]. The splitting of the line into two bumps of *equal* intensity was already discussed for the absorption from only one field [7]. That splitting follows from a thermal phase transition, in which the number of photons of the reservoir increases with increasing temperature, thus, the photons compete with the field for being absorbed at frequencies around the center of the line. Now, in the presence of a pump field the absorption line profile of the probe shows an asymmetry of the heights of the two bumps. Again, this behavior is due to the reservoir density of frequencies $g(\omega)$: if one considers that for one single line the peaks of the bumps are located at $\pm\varepsilon$ from $\omega_{2,0}=\omega_0'$, or more explicitly, at $\omega_{2,\pm}=\omega_1-\sqrt{\Omega^2+(\Delta\omega)^2}\pm\varepsilon$, then

$$g_\pm \equiv g(\omega_{2,\pm}) = \frac{g_0}{1+[\sqrt{\Omega^2+(\Delta\omega)^2}-\Delta\omega\mp\varepsilon]^2\tau^2} \tag{31}$$

shows that $g_+>g_-$; thus, the influence of the reservoir through g_-, at the left bump $(\Delta\nu)_-=-\sqrt{\Omega^2+(\Delta\omega)^2}-\varepsilon$, is less than it is for g_+ at the right bump $(\Delta\nu)_+=-\sqrt{\Omega^2+(\Delta\omega)^2}+\varepsilon$, permitting a higher absorption from the probe at $(\Delta\nu)_-$ than at $(\Delta\nu)_+$. In the limit $(\Omega/\Delta\omega)\rightarrow 0$ we have

$$g_\pm \approx \frac{g_0}{1+(\pm\varepsilon)^2\tau^2}, \tag{32}$$

therefore, the asymmetry disappears and the twin-bumps line profile of [7] is recovered.

In this work we presented several peculiar characteristics in the absorption of the probe field and in the atomic stimulated emission — the imaginary part of the susceptibility function χ'' — when memory effects of the reservoir are taken into account. We considered the steady state of the GME, which describes the dynamics of the atom (imbedded in a reservoir) interacting with two classical fields (pump and probe). New features arise in χ'' when compared with the one calculated from the GME within the MA.

ACKNOWLEDGMENTS

S.S.M. and G.A.P. thank CNPQ, Brazil, for financial support. S.S.M. acknowledges support from Cooperação CNPq-FAPESP, Contract CNPq No. 400285/95-9.

APPENDIX

In this Appendix we determine the time dependence of the matrix density $\rho(t)$ by exploring the features of the expression for the polarization. For a medium composed of noninteracting two-level atoms, which are invariant by spatial inversion, the polarization is highly nonlinear and is written as an odd power series of the field, namely [12],

$$\frac{\mathbf{P}(t)}{\epsilon_0}=\int_{-\infty}^{\infty}dt_1\mathbf{R}^{(1)}(t_1)|\mathbf{E}(t-t_1)+\int_{-\infty}^{\infty}dt_1\int_{-\infty}^{\infty}dt_2\int_{-\infty}^{\infty}dt_3\mathbf{R}^{(3)}(t_1,t_2,t_3)|\mathbf{E}(t-t_1)|\mathbf{E}(t-t_2)|\mathbf{E}(t-t_3)+\cdots. \tag{A1}$$

The response function of the medium, $\mathbf{R}^{(n)}(t_1,\ldots t_n)$, is a tensor of rank $(n+1)$, $\mathbf{E}(t)$ is the applied field, and the vertical bars indicate contraction.

For a single monochromatic field,

$$\mathbf{E}(t)=\boldsymbol{\varepsilon}e^{-i\omega t}+\boldsymbol{\varepsilon}^*e^{i\omega t}, \tag{A2}$$

the integrals in Eq. (A1) provide for the polarization

$$\begin{aligned}\frac{\mathbf{P}(t)}{\epsilon_0}=&\{e^{-i\omega t}[\boldsymbol{\chi}^{(1)}(\omega)|\boldsymbol{\varepsilon}+3\boldsymbol{\chi}^{(3)}(\omega,\omega,-\omega)|\boldsymbol{\varepsilon}\boldsymbol{\varepsilon}\boldsymbol{\varepsilon}^*+10\boldsymbol{\chi}^{(5)}(\omega,\omega,\omega,-\omega,-\omega)|\boldsymbol{\varepsilon}\boldsymbol{\varepsilon}\boldsymbol{\varepsilon}\boldsymbol{\varepsilon}^*\boldsymbol{\varepsilon}^*+\ldots]+\text{c.c.}\}\\&+\{e^{-i3\omega t}[\boldsymbol{\chi}^{(3)}(\omega,\omega,\omega)|\boldsymbol{\varepsilon}\boldsymbol{\varepsilon}\boldsymbol{\varepsilon}+5\boldsymbol{\chi}^{(5)}(\omega,\omega,\omega,\omega,-\omega)|\boldsymbol{\varepsilon}\boldsymbol{\varepsilon}\boldsymbol{\varepsilon}\boldsymbol{\varepsilon}\boldsymbol{\varepsilon}^*+\ldots]+\text{c.c.}\}+\cdots,\end{aligned} \tag{A3}$$

where $\boldsymbol{\chi}^{(n)}$ is the susceptibility tensor of rank $n+1$ and where the intrinsic permutation-symmetry property of the tensor components was used.

Since the macroscopic polarization is defined as

$$\mathbf{P}(t)=N\text{Tr}[\rho(t)\boldsymbol{\mu}], \tag{A4}$$

with N the atomic density, we take for $\rho(t)$ the density matrix for the driven atom, expansion (1), Sec. II, and we obtain in the stationary regime

$$\mathbf{P}(t)=N(\overline{W}_3^{\infty}e^{-i\omega t}\boldsymbol{\mu}_{21}+\text{c.c.}). \tag{A5}$$

Comparing Eq. (A5) with Eq. (A3) we conclude that the nonlinear susceptibilities for which the sum of the frequencies is different from $\pm\omega$ must vanish. Then Eq. (A3) reduces to

$$\frac{\mathbf{P}(t)}{\epsilon_0}=e^{-i\omega t}\overline{\boldsymbol{\chi}}(\omega,\boldsymbol{\varepsilon})\cdot\boldsymbol{\varepsilon}+\text{c.c.}, \tag{A6}$$

where the field-corrected susceptibility $\overline{\boldsymbol{\chi}}$ was introduced.

Now, for the same medium in the presence of two monochromatic fields of different frequencies, the total polarization is obtained by taking

$$\mathbf{E}(t)=\mathbf{E}_1(t)+\mathbf{E}_2(t)=(\boldsymbol{\varepsilon}_1e^{-i\omega_1t}+\boldsymbol{\varepsilon}_2e^{-i\omega_2t})+\text{c.c.} \tag{A7}$$

into Eq. (A1). The field $\mathbf{E}_1(t)$ drives strongly the two-level atoms whereas $\mathbf{E}_2(t)$ is a weak probe field ($|\boldsymbol{\varepsilon}_2|\ll|\boldsymbol{\varepsilon}_1|$) perturbing the stationary state of the driven atoms. Therefore in the expression of the polarization we shall keep terms up to the quadratic power of the perturbing field, like $\boldsymbol{\varepsilon}_2\boldsymbol{\varepsilon}_2^*$, which corresponds to the absorption of only one photon from the probe field,

$$\begin{aligned}\frac{\mathbf{P}(t)}{\epsilon_0}=&(e^{-i\omega_1t}\{\overline{\boldsymbol{\chi}}(\omega_1,\boldsymbol{\varepsilon}_1)|+[6\boldsymbol{\chi}^{(3)}(\omega_1,\omega_2,-\omega_2)|+60\boldsymbol{\chi}^{(5)}\\&\times(\omega_1,\omega_1,-\omega_1,\omega_2,-\omega_2)|\boldsymbol{\varepsilon}_1\boldsymbol{\varepsilon}_1^*+\cdots]\boldsymbol{\varepsilon}_2\boldsymbol{\varepsilon}_2^*\}\boldsymbol{\varepsilon}_1\\&+\text{c.c.})+\{e^{-i(\omega_1+\Delta\nu)t}[6\boldsymbol{\chi}^{(3)}(\omega_2,\omega_1,-\omega_1)|\boldsymbol{\varepsilon}_1\boldsymbol{\varepsilon}_1^*\\&+30\boldsymbol{\chi}^{(5)}(\omega_2,\omega_1,\omega_1,-\omega_1,-\omega_1)|\boldsymbol{\varepsilon}_1\boldsymbol{\varepsilon}_1\boldsymbol{\varepsilon}_1^*\boldsymbol{\varepsilon}_1^*\\&+\cdots]\boldsymbol{\varepsilon}_2+\text{c.c.}\}+\{e^{-i(\omega_1-\Delta\nu)t}\\&\times[3\boldsymbol{\chi}^{(3)}(-\omega_2,\omega_1,\omega_1)|\boldsymbol{\varepsilon}_1\boldsymbol{\varepsilon}_1+20\boldsymbol{\chi}^{(5)}\\&\times(-\omega_2,\omega_1,\omega_1,\omega_1,-\omega_1)|\boldsymbol{\varepsilon}_1\boldsymbol{\varepsilon}_1\boldsymbol{\varepsilon}_1\boldsymbol{\varepsilon}_1^*+\cdots]\\&\times\boldsymbol{\varepsilon}_2^*+\text{c.c.}\},\end{aligned} \tag{A8}$$

where $\Delta\nu=\omega_2-\omega_1$ is the detuning of the probe from the driving field frequency.

To observe more clearly the effect of the probe field and for later use, we cast Eq. (A8) into the following short form

$$\begin{aligned}\frac{\mathbf{P}(t)}{\epsilon_0}=&\{e^{-i\omega_1t}[\overline{\boldsymbol{\chi}}(\omega_1,\boldsymbol{\varepsilon}_1)+\delta\mathbf{A}_0(\omega_1,\omega_2,\boldsymbol{\varepsilon}_1,\boldsymbol{\varepsilon}_2)]\cdot\boldsymbol{\varepsilon}_1+\text{c.c.}\}\\&+[e^{-i(\omega_1+\Delta\nu)t}\delta\mathbf{A}_+(\omega_1,\omega_2,\boldsymbol{\varepsilon}_1)\cdot\boldsymbol{\varepsilon}_2+\text{c.c.}]\\&+[e^{-i(\omega_1-\Delta\nu)t}\delta\mathbf{A}_-^*(\omega_1,\omega_2,\boldsymbol{\varepsilon}_1)\cdot\boldsymbol{\varepsilon}_2^*+\text{c.c.}].\end{aligned} \tag{A9}$$

From Eqs. (A8) and (A9) we verify that the effect of the weak probe field on the stationary state of the driven two-level atom is to induce corrections to the unperturbed polarization and also to introduce additional terms oscillating at frequencies differing by $\pm\Delta\nu$ from the frequency of the unperturbed polarization.

Now, evaluating the macroscopic polarization, Eq. (A4), with $\rho(t)$, the perturbed density matrix, given by Eq. (7), Sec. II, we obtain

$$\mathbf{P}(t)=N\{[\overline{W}_3^{\infty}e^{-i\omega_1t}+\Delta W_3(t)]\boldsymbol{\mu}_{21}+\text{c.c.}\}. \tag{A10}$$

Comparing Eqs. (A9) and (A10) we note that the term $\Delta W_3(t)$ can be written as a sum of three time-dependent contributions:

$$\Delta W_3(t) = \delta W_0 e^{-i\omega_1 t} + \delta W_+ e^{-i(\omega_1+\Delta\nu)t} + \delta W_-^* e^{-i(\omega_1-\Delta\nu)t}; \tag{A11}$$

this form leads us to consider the same structure as the corrections of the other components of $\rho(t)$. Recalling that $\mathrm{Tr}\rho(t)=1$ and $\langle 1|\rho(t)|2\rangle = \langle 2|\rho(t)|1\rangle^*$ we write

$$\begin{aligned} \Delta W_1(t) &= \delta W_1 + \eta e^{-i\Delta\nu t} + \eta^* e^{i\Delta\nu t}, \\ \Delta W_2(t) &= -\delta W_1 - \eta e^{-i\Delta\nu t} - \eta^* e^{i\Delta\nu t}, \\ \Delta W_4(t) &= [\Delta W_3(t)]^*. \end{aligned} \tag{A12}$$

Now we identify the quantities introduced in Eq. (A10):

$$[\bar{\boldsymbol{\chi}}(\omega_1,\boldsymbol{\varepsilon}_1) + \delta\mathbf{A}_0(\omega_1,\omega_2,\boldsymbol{\varepsilon}_1,\boldsymbol{\varepsilon}_2)]\cdot\boldsymbol{\varepsilon}_1 = \frac{N}{\epsilon_0}(\overline{W_3^\infty} + \delta W_0)\boldsymbol{\mu}_{21},$$

$$\delta\mathbf{A}_+(\omega_1,\omega_2,\boldsymbol{\varepsilon}_1)\cdot\boldsymbol{\varepsilon}_2 = \frac{N}{\epsilon_0}\delta W_+ \boldsymbol{\mu}_{21} \tag{A13}$$

$$\delta\mathbf{A}_-^*(\omega_1,\omega_2,\boldsymbol{\varepsilon}_1)\cdot\boldsymbol{\varepsilon}_2^* = \frac{N}{\epsilon_0}\delta W_-^* \boldsymbol{\mu}_{21},$$

from which we obtain the scalar susceptibilities with respect to the fields. Taking the first two equations of Eq. (A13), assuming the medium is isotropic, and averaging them over all directions we have

$$\bar{\chi}(\omega_1,\boldsymbol{\varepsilon}_1) + \delta A_0(\omega_1,\omega_2,\boldsymbol{\varepsilon}_1,\boldsymbol{\varepsilon}_2) = -(\overline{W_3^\infty} + \delta W_0)\frac{N}{\epsilon_0}\frac{|\boldsymbol{\mu}_{12}|^2}{3F_1^*}, \tag{A14}$$

which is the total susceptibility with respect to $\mathbf{E}_1$, and

$$\delta A_+(\omega_1,\omega_2,\boldsymbol{\varepsilon}_1) = -\delta W_+ \frac{N}{\epsilon_0}\frac{|\boldsymbol{\mu}_{12}|^2}{3F_2^*}, \tag{A15}$$

the susceptibility corresponding to the field $\mathbf{E}_2$. In these equations $F_1^* = -\boldsymbol{\mu}_{12}\cdot\boldsymbol{\varepsilon}_1$ and $F_2^* = -\boldsymbol{\mu}_{12}\cdot\boldsymbol{\varepsilon}_2$.

[1] M. Lewenstein, T.W. Mossberg, and R.J. Glauber, Phys. Rev. Lett. **59**, 775 (1987).

[2] A.A. Villaeys, J.C. Vallet, and S.H. Lin, Phys. Rev. A **43**, 5030 (1990).

[3] G. Gangopadhyay and D.S. Ray, Phys. Rev. A **46**, 1507 (1992).

[4] J.P. Lavoine and A.A. Villaeys, Phys. Rev. Lett. **67**, 2780 (1991).

[5] J.P. Lavoine, A.J. Beglin, P. Martin, and A.A. Villaeys, Phys. Rev. B **53**, 11 535 (1996).

[6] J.R. Brinati, S.S. Mizrahi, and G.A. Prataviera, Phys. Rev. A **50**, 3304 (1994).

[7] J.R. Brinati, S.S. Mizrahi, and G.A. Prataviera, Phys. Rev. A **52**, 2804 (1995).

[8] C. Cohen-Tannoudji, J. Dupont-Roc, and G. Grynberg, *Atom-PhotonInteractions* (Wiley-Interscience, New York, 1992).

[9] B.R. Mollow, Phys. Rev. A **5**, 2217 (1972).

[10] F.Y. Wu, S. Ezekiel, M. Ducloy, and B.R. Mollow, Phys. Rev. Lett. **38**, 1077 (1977).

[11] G.S. Agarwal, Phys. Rev. A **19**, 923 (1979).

[12] P.N. Butcher and D. Cotter, *The Elements of Nonlinear Optics*, Cambridge Studies in Modern Optics Vol. 9 (Cambridge University Press, Cambridge, 1993).